Influence of Pseudohalide Anions on Non-Covalent Supramolecular Synthons in Hg(II) complexes with 8-aminoquinoline ligand: DFT Approach and Biological Implications.

Dhrubajyoti Majumdar [a*], Antonio Frontera [b], Jessica Elizabeth Philip [c], Bouzid Gassoumi [d], Sergi Burguera [b], Sourav Roy [e], Sahbi Ayachi [f]

[a] Department of Chemistry, Tamralipta Mahavidyalaya, Tamluk-721636, West Bengal, India.

[b] Department de Quimica, Universitat de les Illes Balears, Crta. de Valldemossa km 7.5. 07122 Palma de Mallorca (Baleares), Spain.

[c] Department of Chemistry, St. George's College, Aruvithura, Kottayam, Kerala-686122, India.

[d] Laboratory of Advanced Materials and Interfaces (LIMA), Faculty of Sciences of Monastir, Avenue of Environment, University of Monastir, 5000 Monastir, Tunisia.

[e] Solid State and Structural Chemistry Unit, Indian Institute of Science, Bangalore 560 012, India.

[f] Laboratory of Physico-Chemistry of Materials (LR01ES19), Faculty of Sciences, University of Monastir, Avenue of the Environment 5019 Monastir, Tunisia.

Corresponding author EMAIL: dmajumdar30@gmail.com, toni.frontera@uib.es.

Contents of Electronic Supporting Materials

Section S1: Experimental of Disk diffusion method.

The disc diffusion method was used to assess the antimicrobial activity of the Hg (II) complexes. Cephalothin, chloramphenicol, and cycloheximide were positive controls for Gram-positive and Gram-negative bacteria and fungi. Nutrient agar was prepared, autoclaved at 121°C for 15 minutes, cooled, and poured into Petri dishes. The compounds were dissolved in dimethyl sulfoxide (DMSO) to prepare 100 and 50 mg/mL concentrations. A 10 µL volume of each preparation was applied to 6 mm diameter disks, resulting in final concentrations of 1 and 0.5 mg/disk, respectively. Bacterial cultures were grown in nutrient broth at 30°C. After 16 hours, each microorganism, at a concentration of 10^8 cells/mL, was inoculated onto the surface of Mueller–Hinton agar plates using a sterile cotton swab. Filter paper disks (6 mm in diameter) were then impregnated with 10 µL of each dissolved compound and placed on the inoculated plates. The plates were incubated at 36°C for 24 hours. Three replicates were performed for each extract and test organism, including a solvent-only negative control. After incubation, the inhibition zones around each disk were measured in millimetres using a transparent ruler, averaged, and recorded.

Section S2: Resazurin Microdilution Assay.

The antimicrobial activity of Hg compounds was assessed using the Resazurin Microdilution Assay (RMDA). [The assay was performed in 96-well microtiter plates (HiMedia) under controlled conditions. In the first row, 100 µL of the test compounds dissolved in sterile water was added, while all wells were filled with 50 µL of Luria broth. A two-fold serial dilution was then performed by transferring 50 µL from the first row to subsequent rows, creating a range of concentrations. Each well was supplemented with 2 µL of resazurin solution as a growth indicator and 10 µL of microbial suspension, resulting in a final concentration of 5×10^6 CFU/mL. Three controls were included on each plate: (a) Cephalothin as a positive control, (b) wells with all reagents except the test compound, and (c) wells where microbial suspension

was replaced by 10 μL of Luria broth. The plates were incubated at 37°C for 24 hours, and colour changes were monitored. A shift from purple to pink or colourless signalled microbial growth, and the MIC was determined as the lowest concentration with no colour change.

Section S3: Cytotoxicity MTT Assay.

H9c2 and HepG2 cells were cultured in Dulbecco's Modified Eagle's Medium (DME) and [seeded into 96-well plates at a density of 5×10^3 cells per well. The plates were incubated at 37°C with 5% CO_2 for 24 hours before adding test samples. The cells were then treated with different concentrations (1, 5, 10, and 25 μM) of the compounds dissolved in DMSO and incubated at 37°C with 5% CO_2 for 24 hours. Each experiment was performed in triplicate. After the 24-hour treatment, MTT solution was added to the wells (following media removal) at a concentration of 50 μg per well, and the plates were incubated in a CO_2 incubator. The MTT solution was prepared in Hank's balanced salt solution (HBSS) without phenol red. After 3 hours, the resulting formazan crystals were observed under a contrast microscope. The crystals were then dissolved by adding DMSO (after removing the MTT solution), followed by a 20-minute incubation at 37°C. The absorbance was measured at 570 nm to assess cell viability.

Section S4: Principle of Hirshfeld Surface.

To gain a comprehensive understanding of the intra- and intermolecular interactions that contribute to the stability of complex, Hirsfeld surface analysis is employed. [S1,S2] This technique is particularly effective for visualizing interactions using color coding. Interactions characterized by distances greater than, equal to, and less than sum of van der Waals radii are indicated by red, while, and blue color regions on the HS respectively. The predominant forces responsible for the stability of both studied complexes have been analyzed with 2D-fingerprint plots. This tool quantifies the contribution of each intermolecular contact as a percentage of the total HS area.

Section S5: Principle of NLO analysis.

The NLO properties of the studied compounds, **1** and **2**, were analyzed and compared to those of urea, a widely used reference molecule in NLO research. [S3,S4] The calculated NLO parameters are presented in Table 4, and some parameters are computed using the following equations:

$$\mu_{tot} = \sqrt{(\mu_x{}^2 + \mu_y{}^2 + \mu_z{}^2)} \quad (1)$$

$$\alpha_{ISO} = \frac{1}{3}(\alpha_{xx} + \alpha_{yy} + \alpha_{zz}) \quad (2)$$

$$\alpha_{ANISO} = \frac{1}{\sqrt{2}}[(\alpha_{xx} - \alpha_{yy})^2 + (\alpha_{xx} - \alpha_{zz})^2 + (\alpha_{zz} - \alpha_{yy})^2 + 6(\alpha_{yz}{}^2 + \alpha_{xz}{}^2 + \alpha_{xy}{}^2)]^{1/2} \quad (3)$$

$$\beta_0 = [(\beta_{xxx} + \beta_{xyy} + \beta_{xzz})^2 + (\beta_{xxy} + \beta_{yyy} + \beta_{yzz})^2 + (\beta_{xxz} + \beta_{zyy} + \beta_{zzz})^2]^{1/2} \quad (4)$$

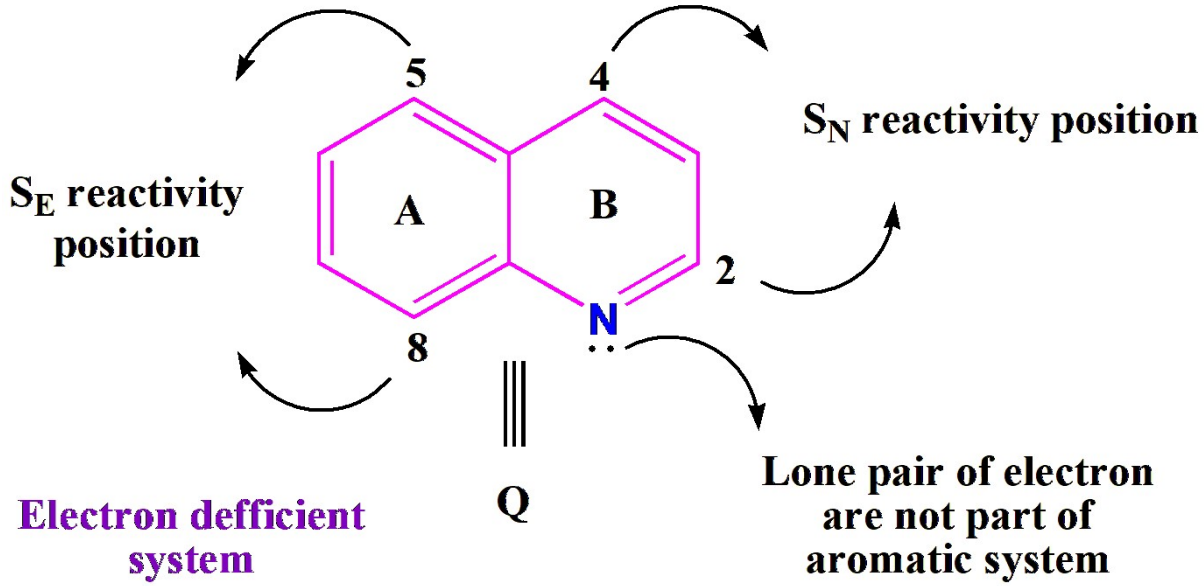

Complexing Activities of Q (Quinoline) Moiety.

Q Salient features

1. ***Ring N takes part for metal complex formation***
2. ***Supramolecular π-π stacking interactions***
3. ***Metal complexes planar and stable***
4. ***Ring N assisted extra coordination site for complex formation***

SCHEME S1 Importance of Quinoline (Q) moiety in 8-aq. [S5]

Table S1 Complexes crystal data and structure refinement parameters.

Identification code	**1**	**2**
Empirical formula	$C_{10}H_8ClHgN_3S$	$C_{10}H_8ClHgN_3Se$
Formula weight	438.29	485.19
Temperature/K	296.15	298(2)
Crystal system	monoclinic	monoclinic
Space group	$P2_1/c$	$P2_1/c$
a/Å	10.5813(19)	10.780(17)
b/Å	14.597(3)	14.69(2)
c/Å	7.8316(14)	7.948(12)
α/°	90	90
β/°	105.946(4)	106.55(4)
γ/°	90	90
Volume/Å^3	1163.1(4)	1206(3)
Z	4	4
ρ_{calc}g/cm^3	2.503	2.672
μ/mm^{-1}	13.615	15.972
F(000)	808.0	880.0
Crystal size/mm^3	0.1 × 0.08 × 0.05	0.3 × 0.24 × 0.02
Radiation	MoKα (λ = 0.71073)	MoKα (λ = 0.71073)
2Θ range for data collection/°	4.004 to 50.378	3.942 to 50.702
Index ranges	-12 ≤ h ≤ 12, -17 ≤ k ≤ 17, -9 ≤ l ≤ 9	-12 ≤ h ≤ 12, -17 ≤ k ≤ 17, -9 ≤ l ≤ 9
Reflections collected	34880	37667
Independent reflections	2076 [R_{int} = 0.2062, R_{sigma} = 0.0666]	2174 [R_{int} = 0.1609, R_{sigma} = 0.0664]
Data/restraints/parameters	2076/0/145	2174/0/146
Goodness-of-fit on F^2	0.932	1.022
Final R indexes [I>=2σ (I)]	R_1 = 0.0418, wR_2 = 0.1066	R_1 = 0.0440, wR_2 = 0.1034
Final R indexes [all data]	R_1 = 0.0603, wR_2 = 0.1127	R_1 = 0.0744, wR_2 = 0.1214
Largest diff. peak/hole / e Å^{-3}	1.69/-2.13	1.48/-1.65

Table S2 Selected distances **(**Å) and angles **(°)** experimental vs. computed at the DFT/B3LYP-D3/LanL2DZ level of theory.

Complex 1		
Bond length	**Experimental**	**DFT**
Hg1-S1	2.507(3)	2.628
Hg1-Cl1	2.560(4)	2.531

Hg1-N2	2.322(9)	2.504
Hg1-N1	2.346(9)	2.602
Bond Angles		
Se1-Hg1-Cl1	114.43(10)	149.729
N2-Hg1-Cl1	101.92(19)	109.495
N2-Hg1-S1	131.48(19)	118.370
N2-Hg1-N1	73.7(3)	66.463
N1-Hg1-Cl1	95.8(2)	84.624
N1-Hg1-S1	129.5(2)	118.370

Complex 2		
Bond length	**Experimental**	**DFT**
Hg1-Se1	2.394(3)	2.750
Hg1-Cl1	2.539(2)	2.513
Hg1-N2	2.297(7)	2.517
Hg1-N1	2.346(7)	2.588
Bond Angles		
Se1-Hg1-Cl1	114.60(12)	144.727
N2-Hg1-Cl1	102.0(2)	107.059
N2-Hg1-Se1	131.7(2)	102.796
N2-Hg1-N1	73.3(3)	66.295
N1-Hg1-Cl1	95.3(3)	107.283
N1-Hg1-Se1	129.5(2)	102.796

Table S3 Hydrogen bond distances (Å) and angles (°) of complexes **1 & 2**.

D-H···A	D-H	H···A	D···A	∠D-H···A
Complex 1				
N(1)-H(1A)···N(3)[a]	0.89	2.35	3.049(13)	136
N(1)-H(1B)···Cl(1)[b]	0.89	2.45	3.334(7)	172
C(8)-H(8)···Cl(1)[c]	0.93	2.67	3.537(10)	155
Complex 2				
N(1)-H(1A)···N(3)[a]	0.89	2.40	3.126(16)	138
N(1)-H(1B)···Cl(1)[b]	0.89	2.47	3.351(11)	170
C(8)-H(8)···Cl(1)[c]	0.93	2.70	3.567(13)	156

D = donor; H = hydrogen; A = acceptor. [a]= x, y,1+z, [b]= x,1/2-y,1/2+z, [c]= x,1/2-y, 1/2+z.

Table S4 EDX data.

Spectrum 1								
Element	Line Type	Apparent Concentration	K Ratio	Wt %	Wt % Sigma	Atomic C %	Standard Label	Factory Standard
C	K series	0.04	0.00038	45.02	1.17	74.17	C Vit	Yes
N	K series	0.03	0.00006	11.64	1.35	16.44	BN	Yes
S	K series	0.04	0.00033	9.86	0.47	6.08	FeS2	Yes
Hg	M series	0.10	0.00094	33.49	1.15	3.30	HgTe	Yes
Total				100.00		100.00		

Table S5 XYZ coordinate of the complex **1.**

Number	Symbol	X	Y	Z
1	Hg	1.4376810	0.0407330	-0.0355280
2	Cl	2.9145660	-1.7698250	0.9379510
3	S	1.1892310	2.3441910	-1.2777650
4	N	-0.7936860	0.0009850	1.1020960
5	N	-0.0763570	-1.9386370	-0.7859710
6	H	0.1580490	-2.3899580	-1.6667410
7	H	0.3316950	-2.4333720	0.0111160
8	C	-1.7964850	-0.5825170	0.3491350
9	C	-1.1152160	0.8924610	2.0482600
10	H	-0.2917710	1.3442440	2.5937450
11	C	-3.1695650	-0.1985870	0.5164780
12	C	-1.4509710	-1.5514070	-0.6525110
13	C	-2.4565180	1.2727860	2.3232640
14	H	-2.6557270	1.9985370	3.1042060
15	C	-3.4748540	0.7424530	1.5442650
16	H	-4.5064280	1.0517340	1.6921810
17	C	-2.4442080	-2.0465810	-1.4926930
18	H	-2.1855590	-2.7734080	-2.2596810
19	C	-4.1640790	-0.7392480	-0.3516470
20	H	-5.1998370	-0.4337170	-0.2282060
21	N	-1.7280990	2.4521030	-0.9983240
22	C	-3.7992880	-1.6294870	-1.3513340
23	H	-4.5485580	-2.0319950	-2.0272070
24	C	-0.5462560	2.4048110	-1.1169990

Table S6 XYZ coordinate of the complex **2.**

Number	Symbol	X	Y	Z
1	Se	-2.9200050	-1.1595760	0.1627270
2	Cl	-0.3525170	3.1478880	0.3100050
3	N	1.0647230	-0.6008280	0.8642140
4	N	0.6027730	-0.2065080	-1.8613890
5	C	2.1602660	-0.4812730	0.0296130
6	C	1.9499650	-0.2034280	-1.3630940
7	C	3.4990510	-0.5973070	0.5376510
8	C	3.6540690	-0.9500540	1.9138230
9	C	3.0491340	0.0596480	-2.1750910
10	C	2.5340100	-1.1362220	2.7135950
11	C	4.6036230	-0.3452910	-0.3301490
12	C	1.2438190	-0.9203810	2.1503170
13	C	4.3745700	0.0052910	-1.6539470

14	C	-1.7917380	-2.2663600	-0.8382730
15	N	-1.0227180	-2.8980380	-1.4924880
16	H	0.1701930	-1.1390470	-1.8602920
17	H	0.4927210	0.2585470	-2.7601010
18	H	4.6547910	-1.0621510	2.3241400
19	H	2.8978210	0.2829540	-3.2286170
20	H	2.6210930	-1.4097110	3.7597170
21	H	5.6158000	-0.4257630	0.0580410
22	H	0.3507940	-0.9915400	2.7644820
23	H	5.2097890	0.2142510	-2.3165110

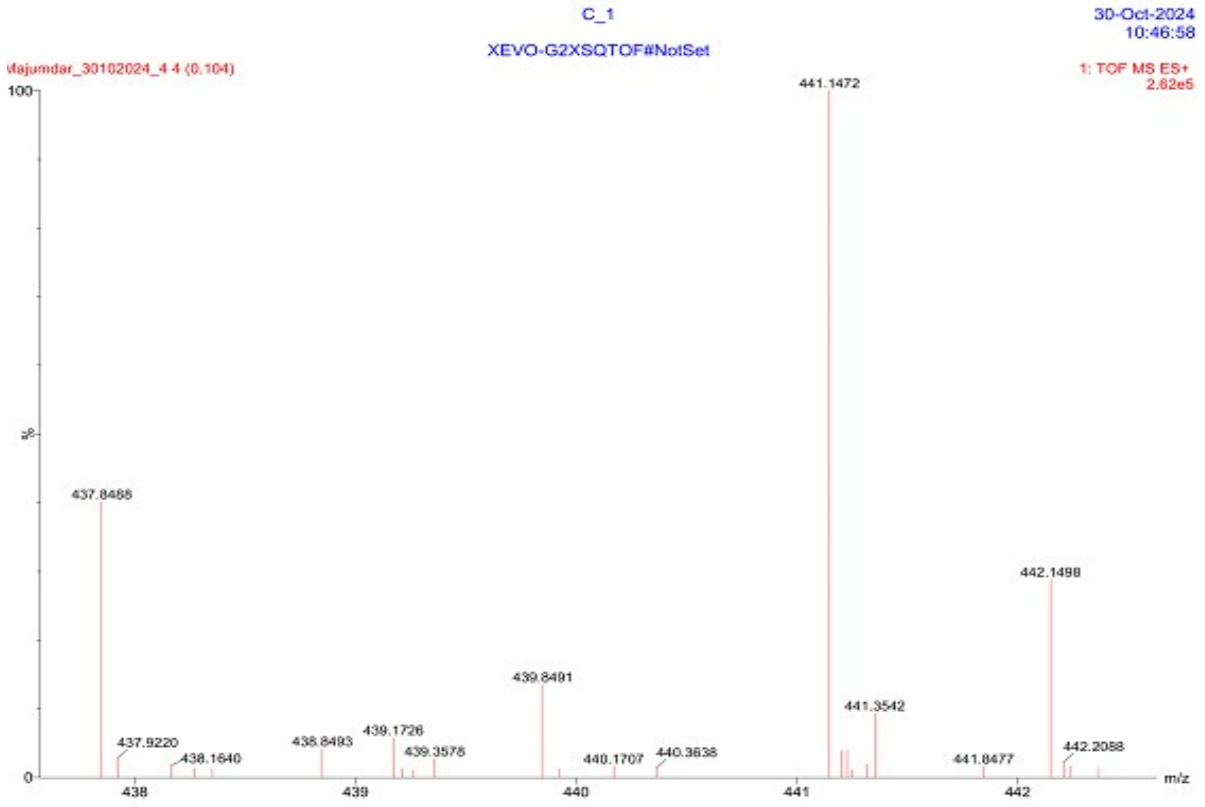

S1

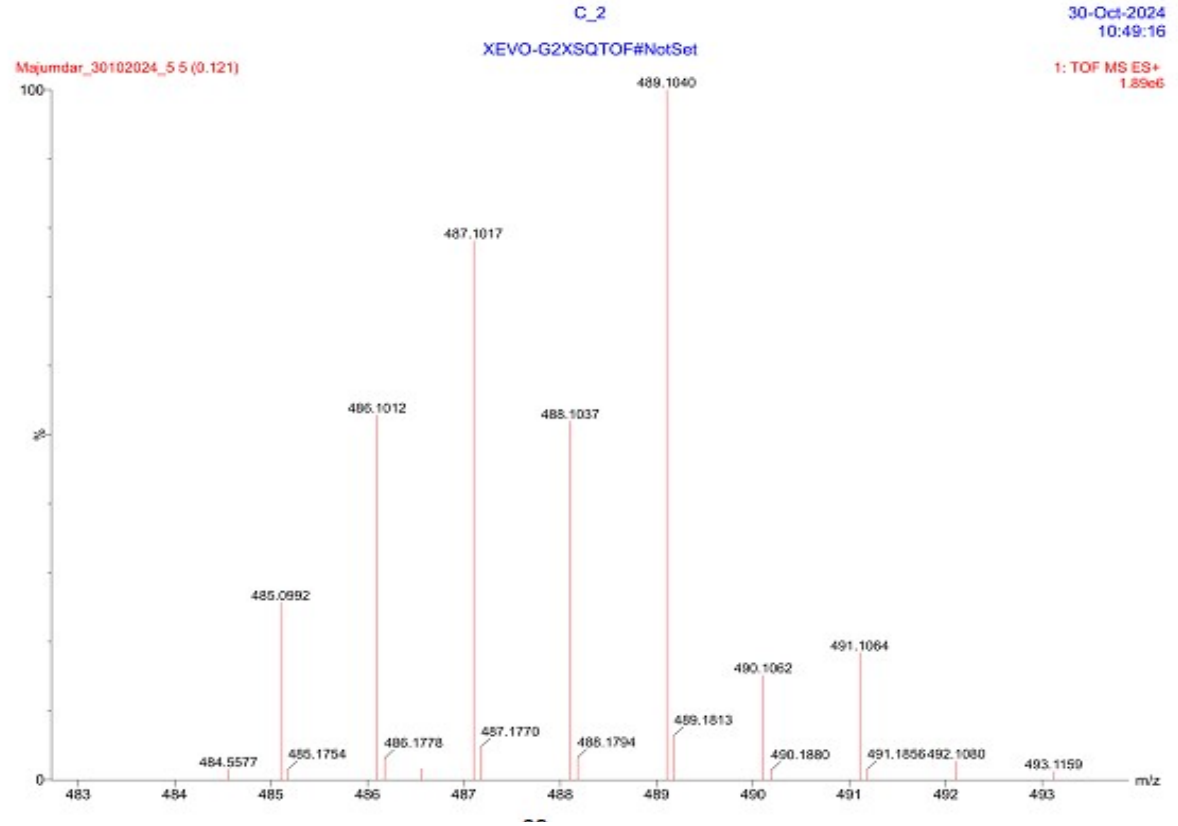

Fig.S1-S2 HRMS for the complex **1** & **2**.

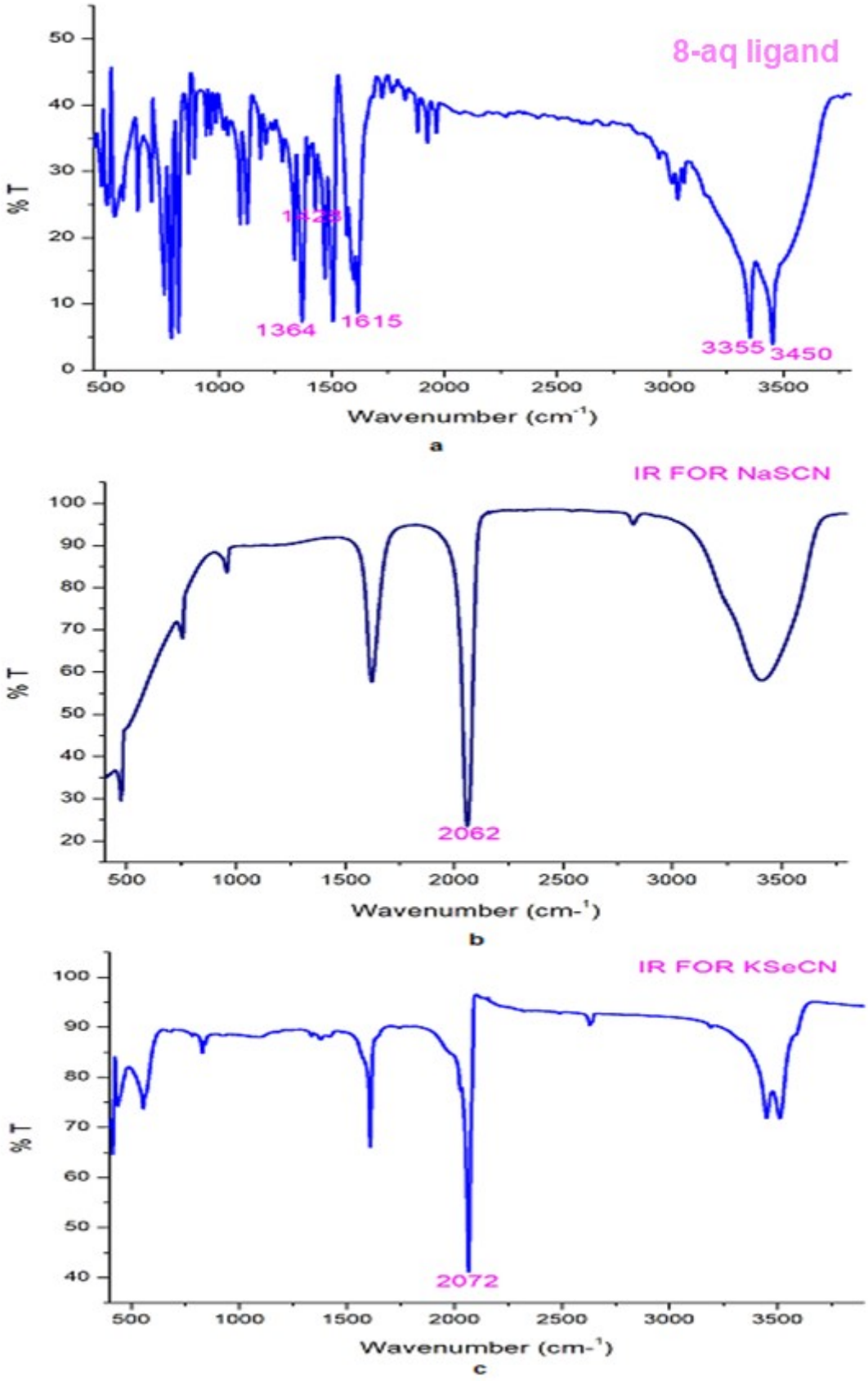

Fig.S3a-c IR spectrum for 8-aq, NaSCN, and KSeCN.

Additional From Fig.S3a-c, the IR spectral data for 8-aq, SCN^- and $SeCN^-$ are listed below:

1. For 8-aq, IR spectral data: ν(N-H), 3355-3500, ν(C□C), 1615, ν(phenyl ring), 1428, 1364, (Fig.S3a).

2. For SCN, IR spectral data: ν(NaSCN), 2062 (Fig.S3b).

2. For SeCN, IR spectral data: ν(SeCN), 2127 s, (Fig.S3c).

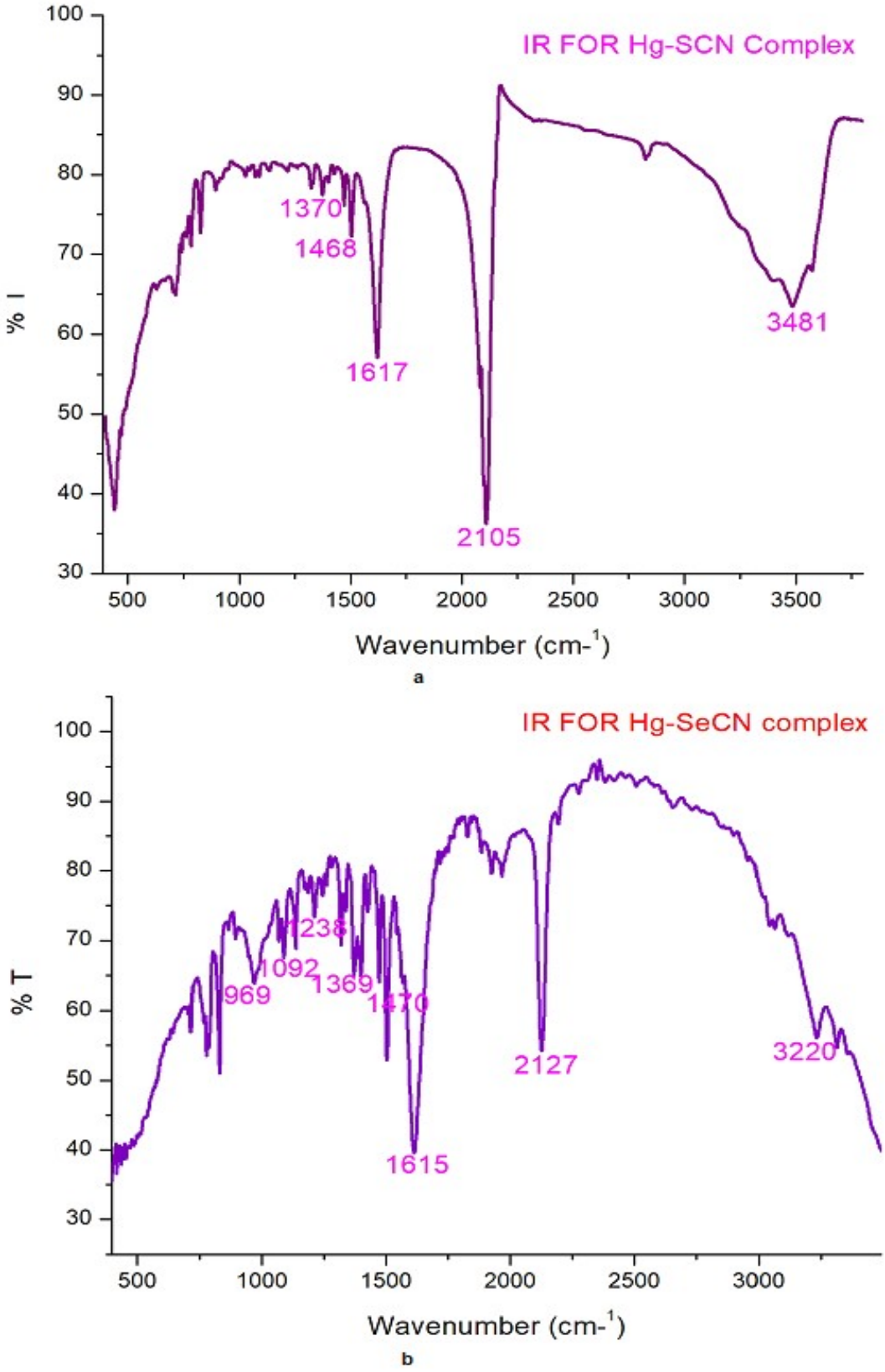

Fig.S4a-b IR spectrum for the complex **1** and **2.**

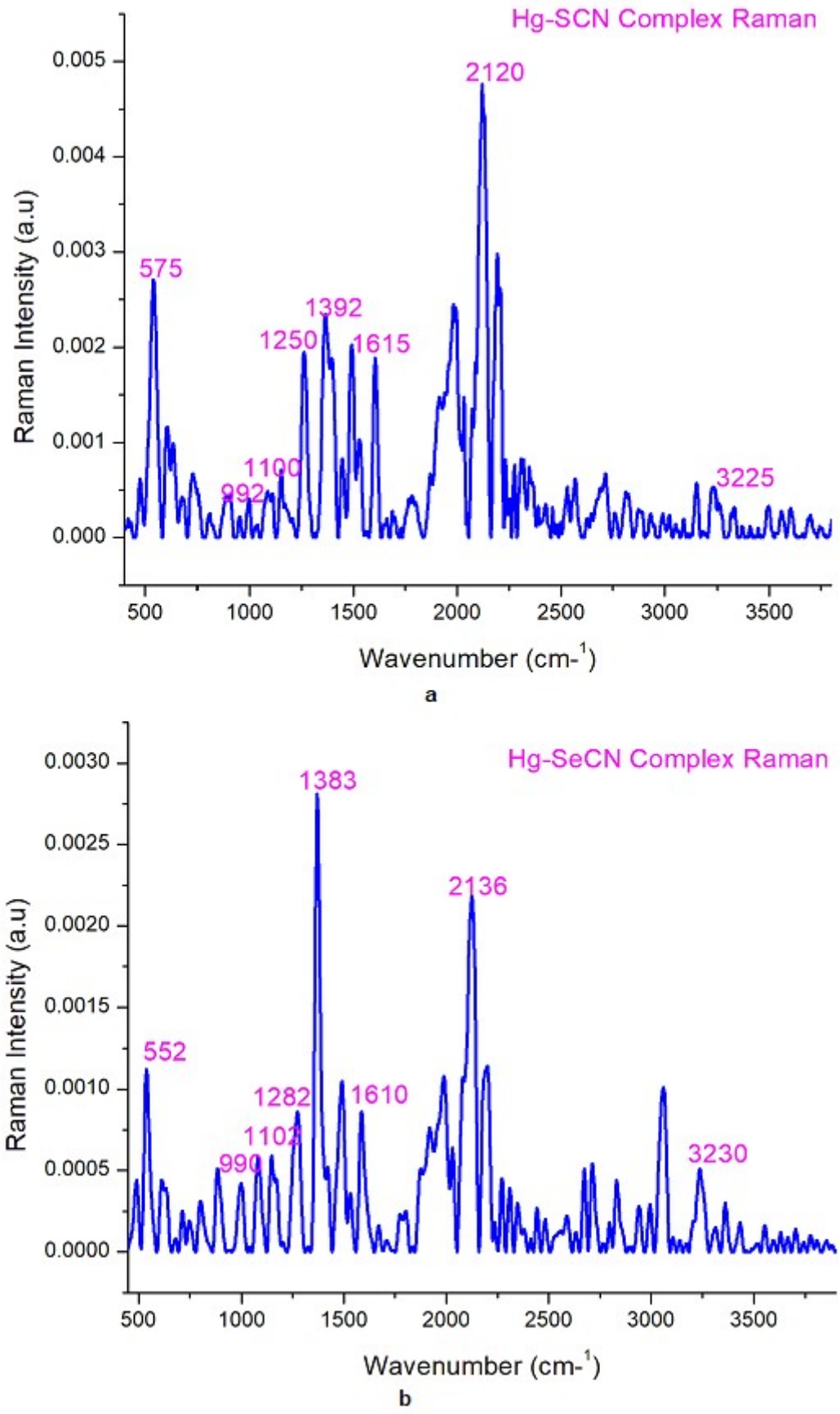

Fig.S5a-b Raman spectrum for the complex **1** and **2.**

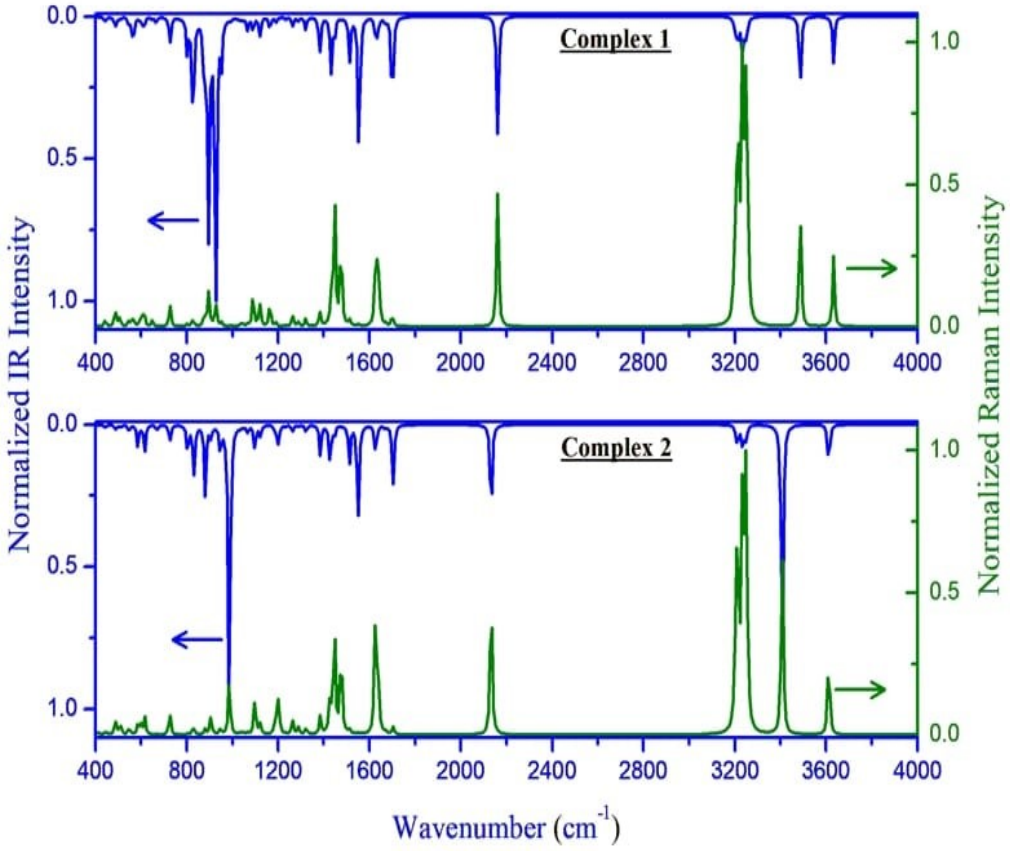

Fig.S5c. Theoretical Raman and FT-IR spectra of the studied Hg(II) complex.

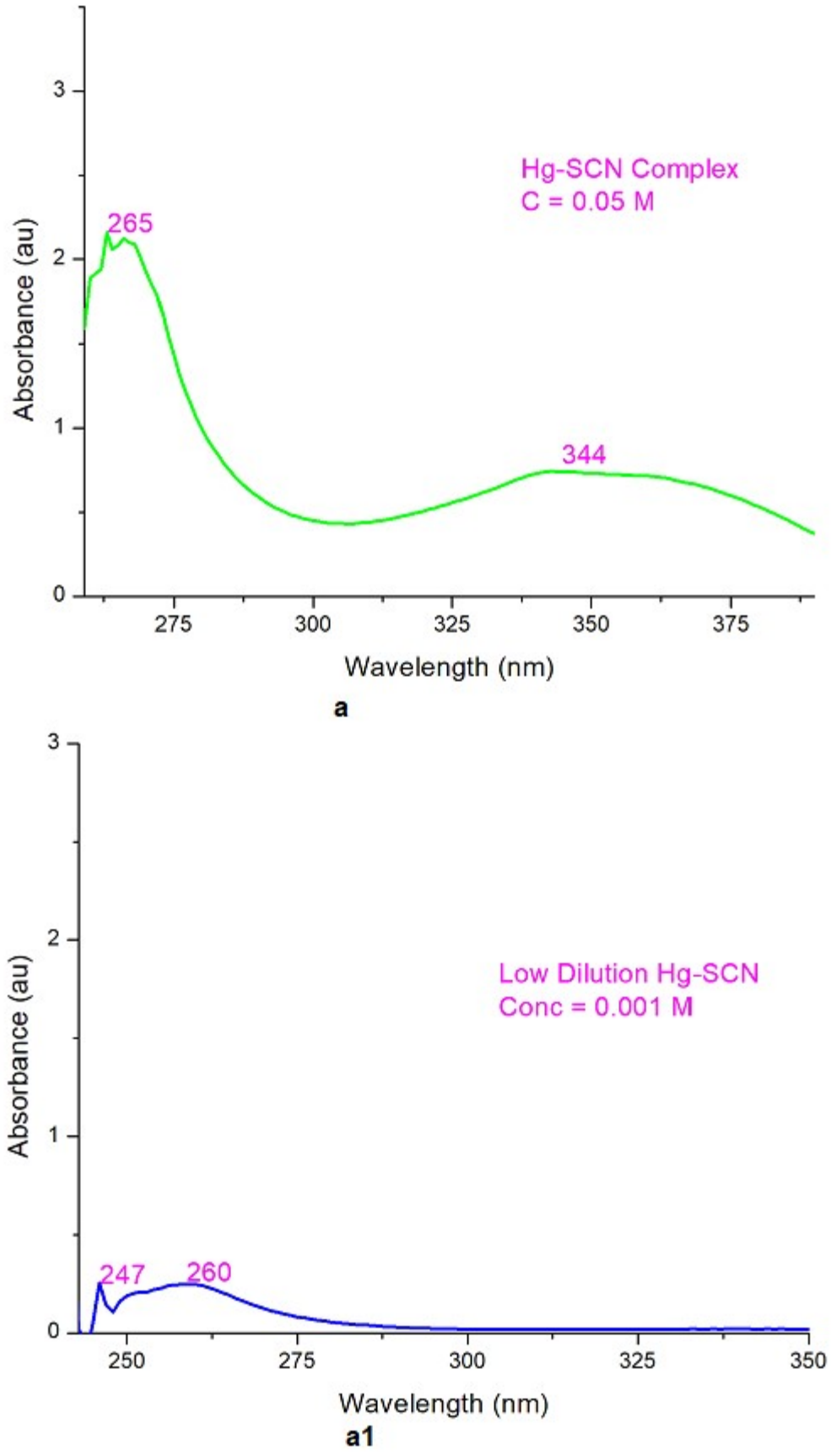

Fig.S6a-a1. UV-VIS spectrum (High-Low Conc.) for the complex **1.**

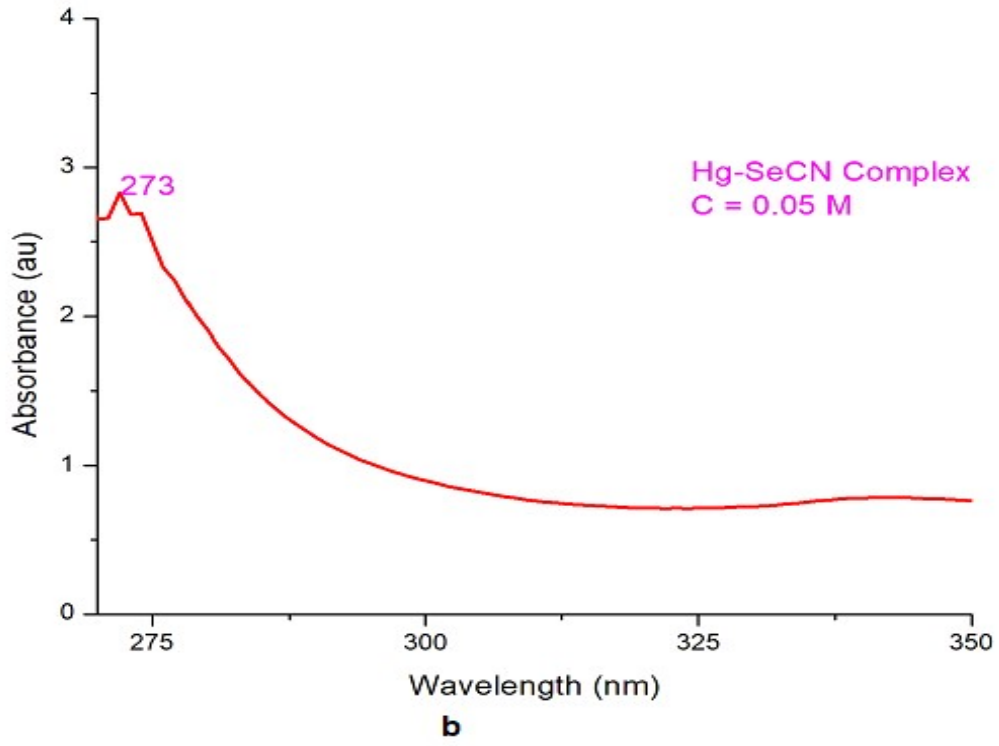

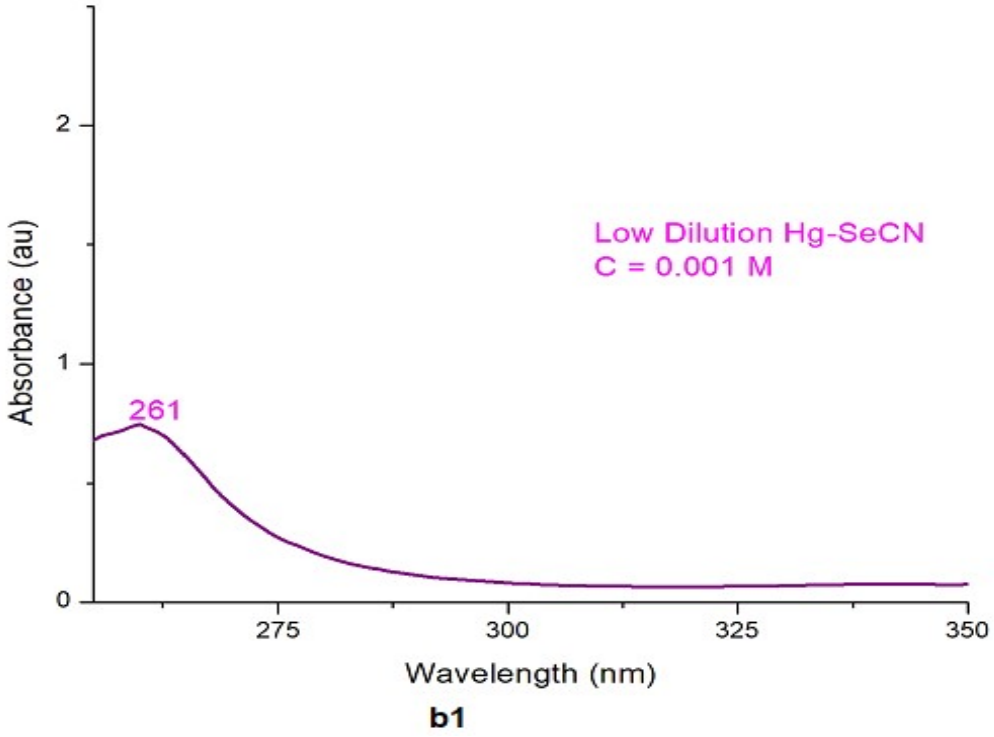

Fig.S6b-b1. UV-VIS spectrum (High-Low Conc.) for the complex **2.**

<u>Additional low dilution (0.001M) UV-VIS spectrum</u>

For Hg-SCN complex, λ_{max} 247 nm (ε = 299 M^{-1} cm^{-1}) and λ_{max} 260 nm (ε = 258 M^{-1} cm^{-1}).

For Hg-SeCN complex, λ_{max} 261 nm (ε = 766 M^{-1} cm^{-1}).

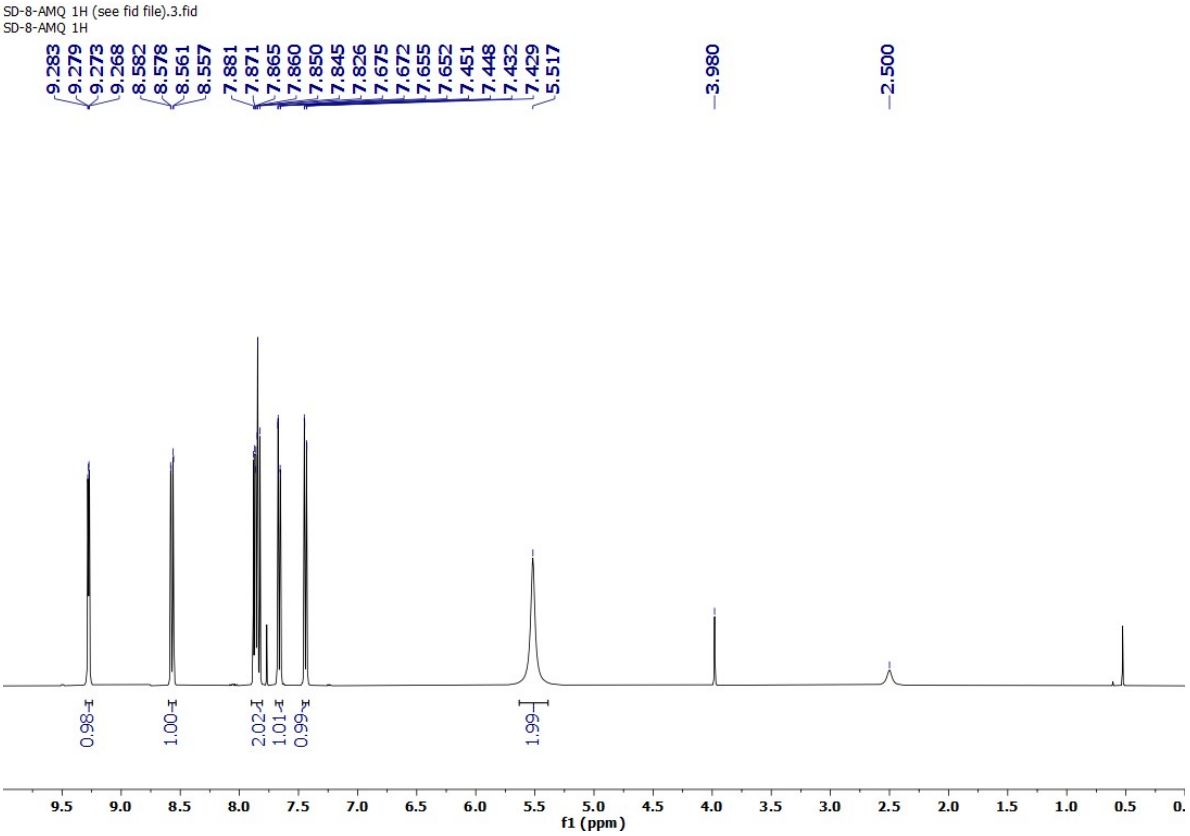

^{1}H NMR (400 MHz, d_6-DMSO, ppm): δ 9.27 (1H, dd, J = 4.4, 2 Hz), 8.56 (1H, dd, J = 8.4, 1.6 Hz), 7.85 (2H, m), 7.66 (1H, dd, J = 8, 1.2 Hz), 7.44 (1H, dd, J = 7.6, 1.2 Hz), 5.51 (2H, br, s).

Fig.S7a ^{1}H NMR spectra for 8-aq.

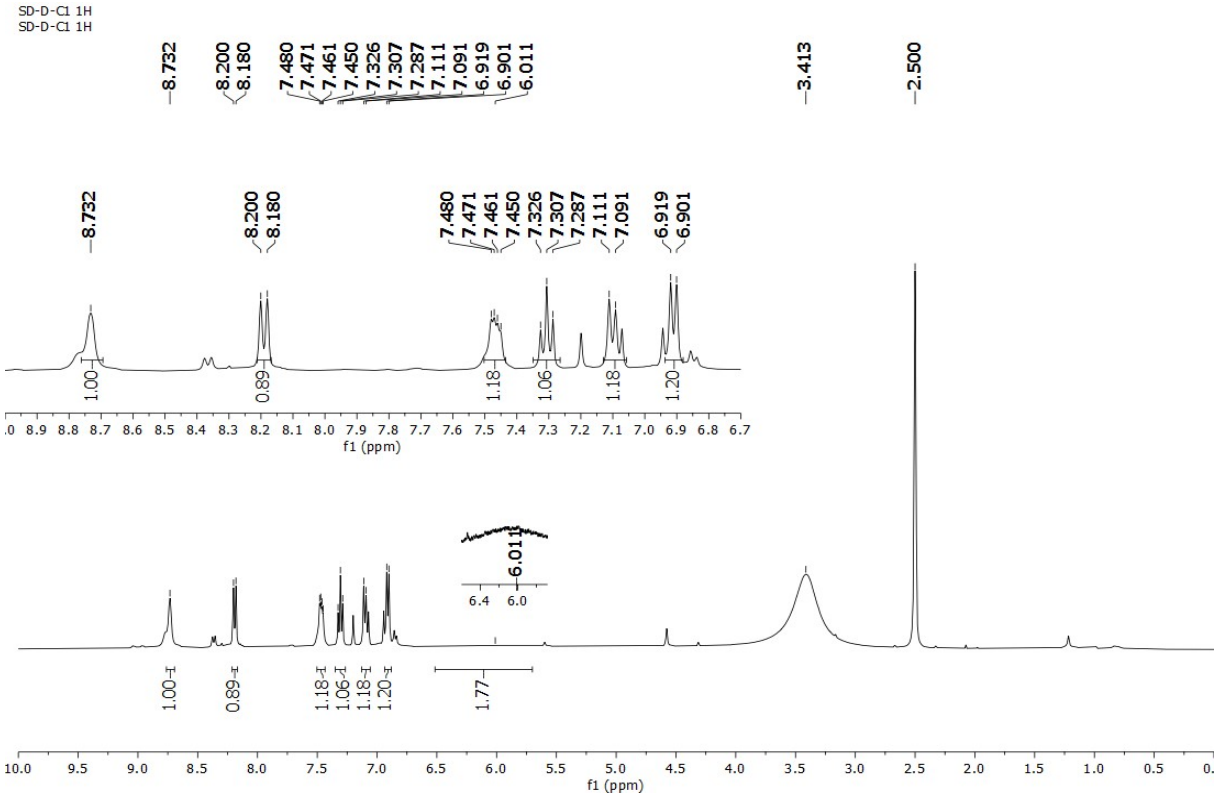

Fig.S7b [1]H NMR spectra for complex **1**.

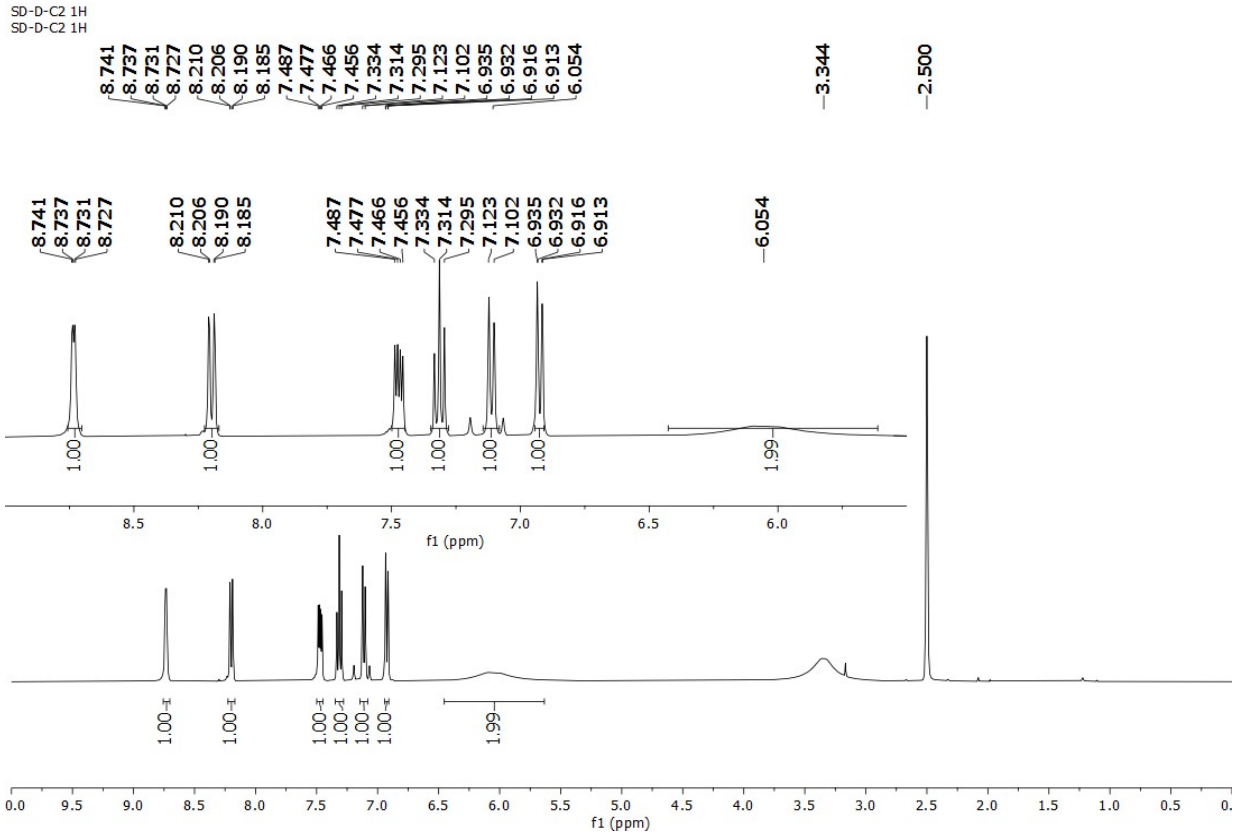

Fig.S7c [1]H NMR spectra for complex **2**.

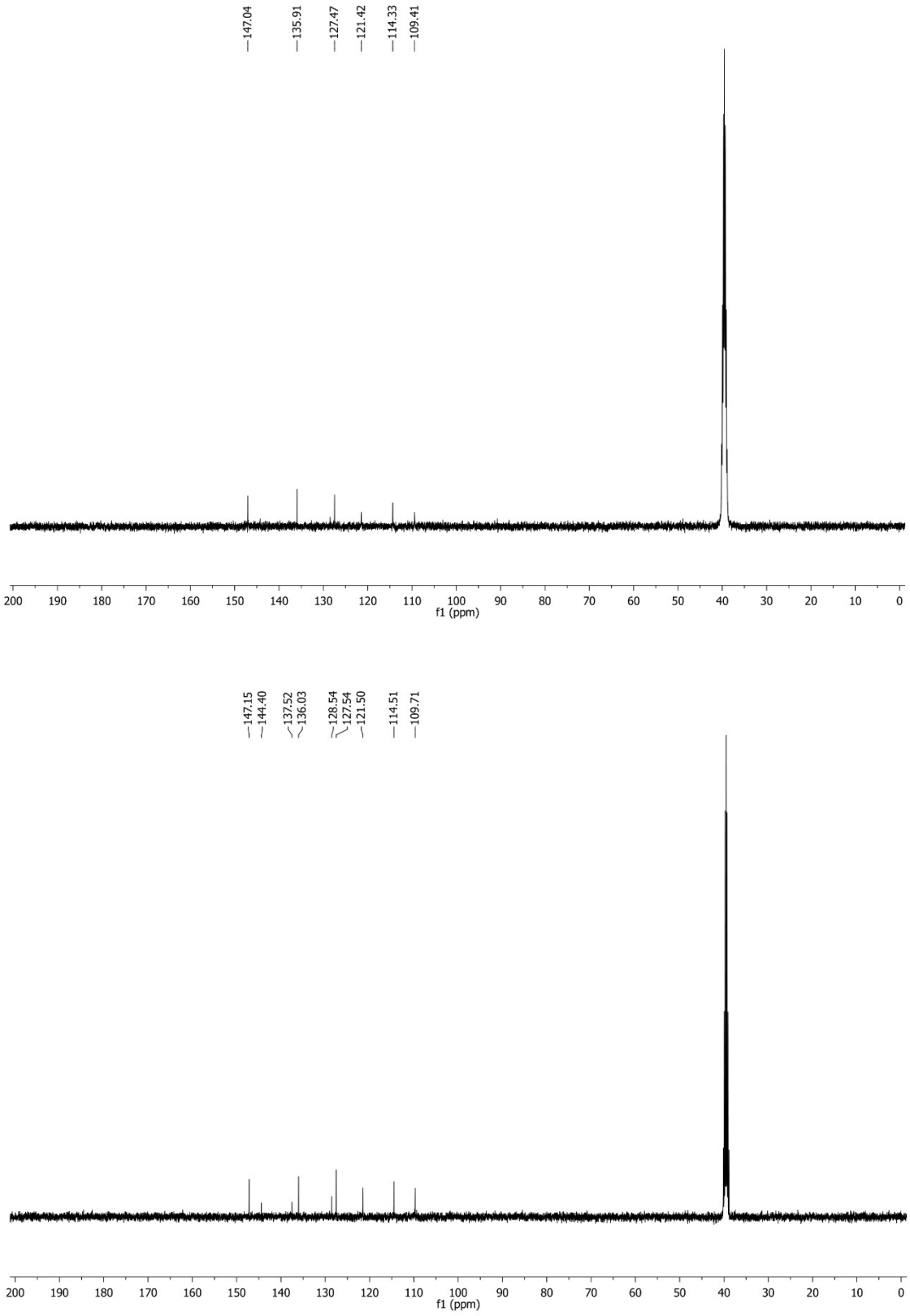

Fig.S8a-b ^{13}C NMR spectra for complex **1** and **2**.

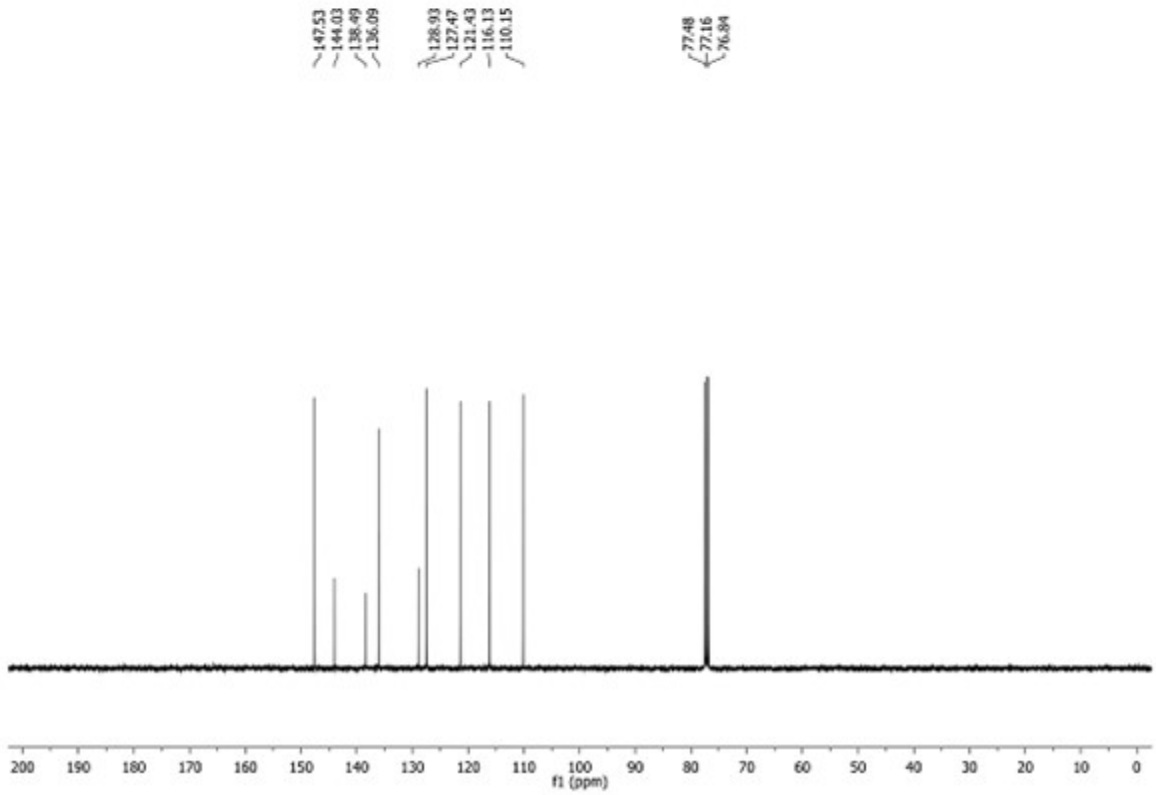

Fig.S8b1. ^{13}C NMR spectra for 8-aq ligand.

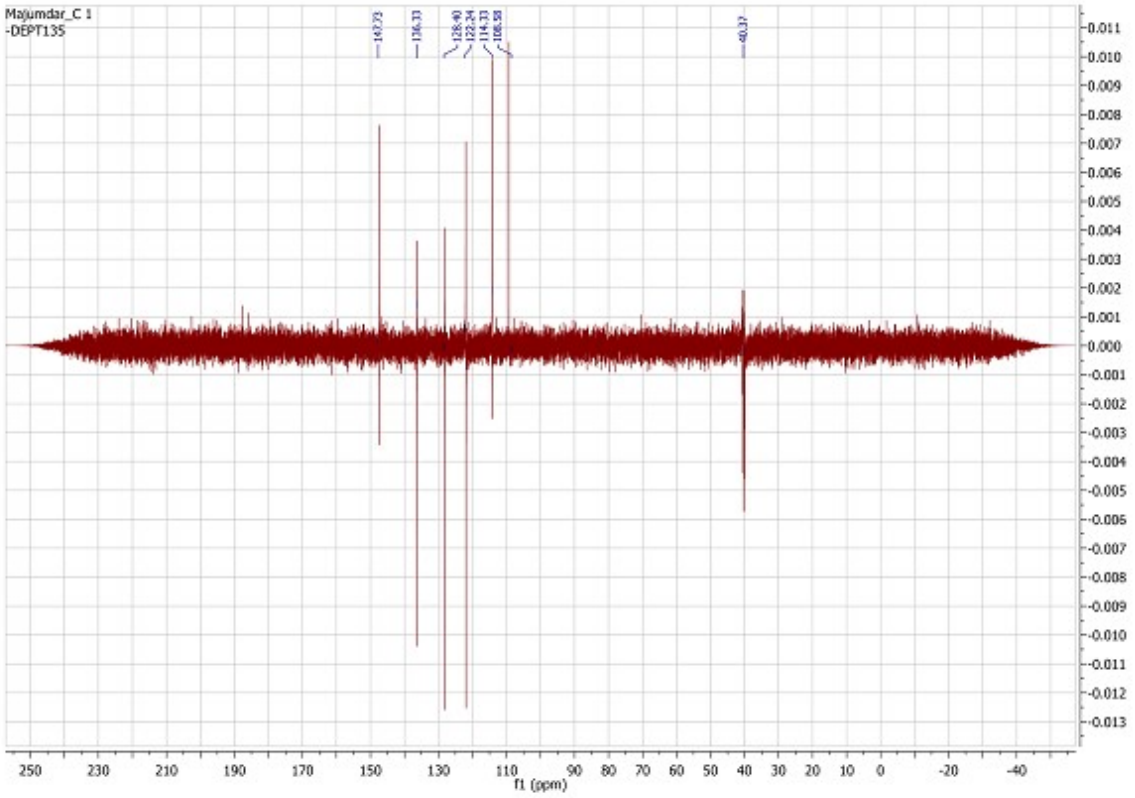

a

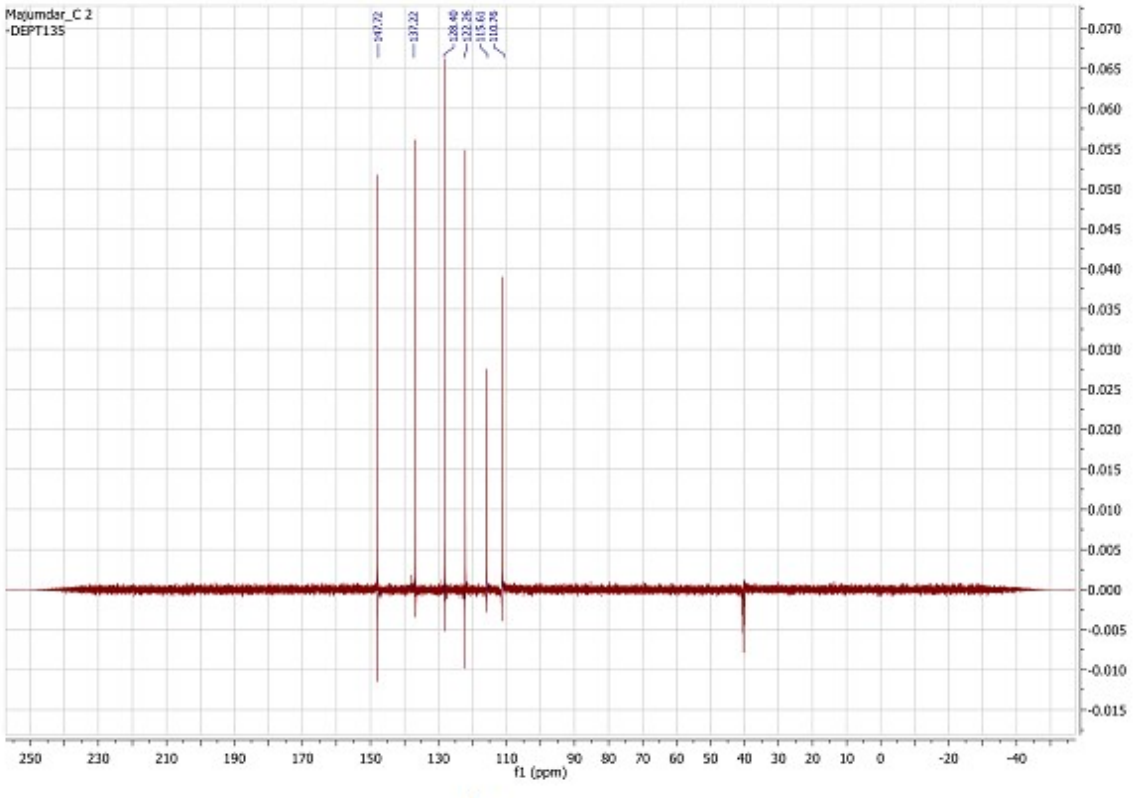

b

Fig.S9a-b ^{13}C DEPT NMR spectra for complex **1** and **2**.

12/03/2024

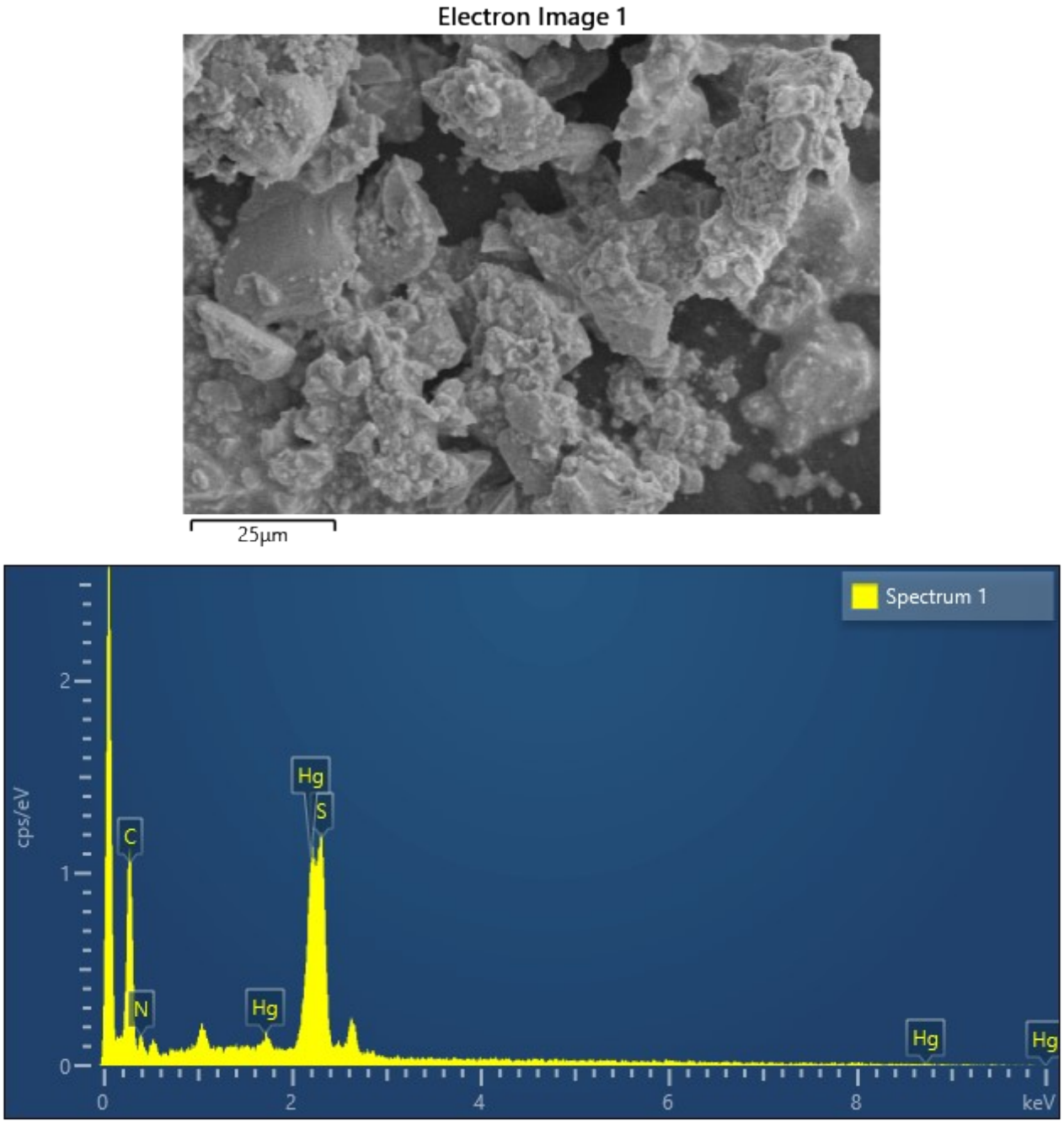

Fig.S10 EDX profile for complex **1**.

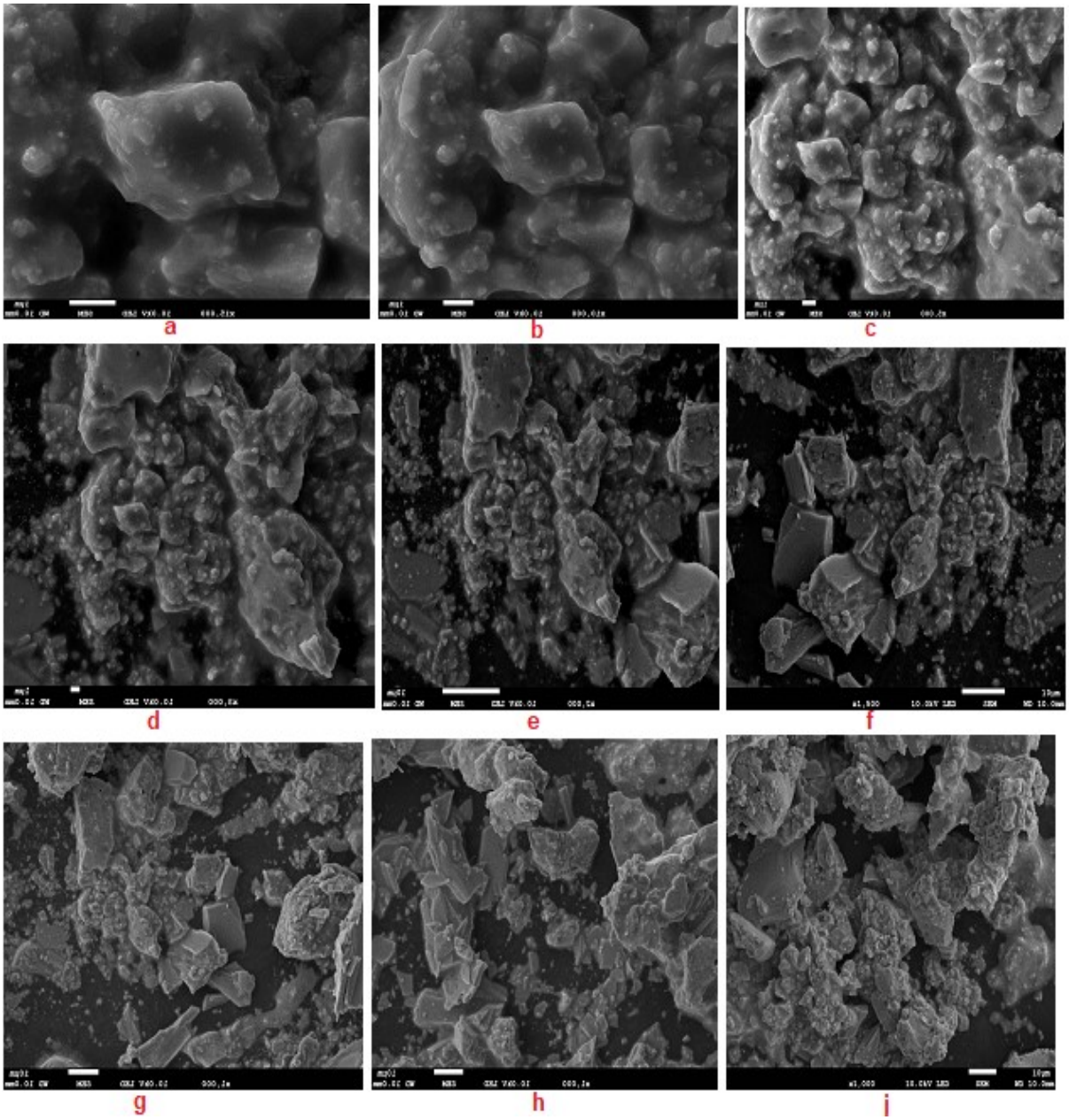

Fig.S11a-j SEM micrographs for complex **1**.

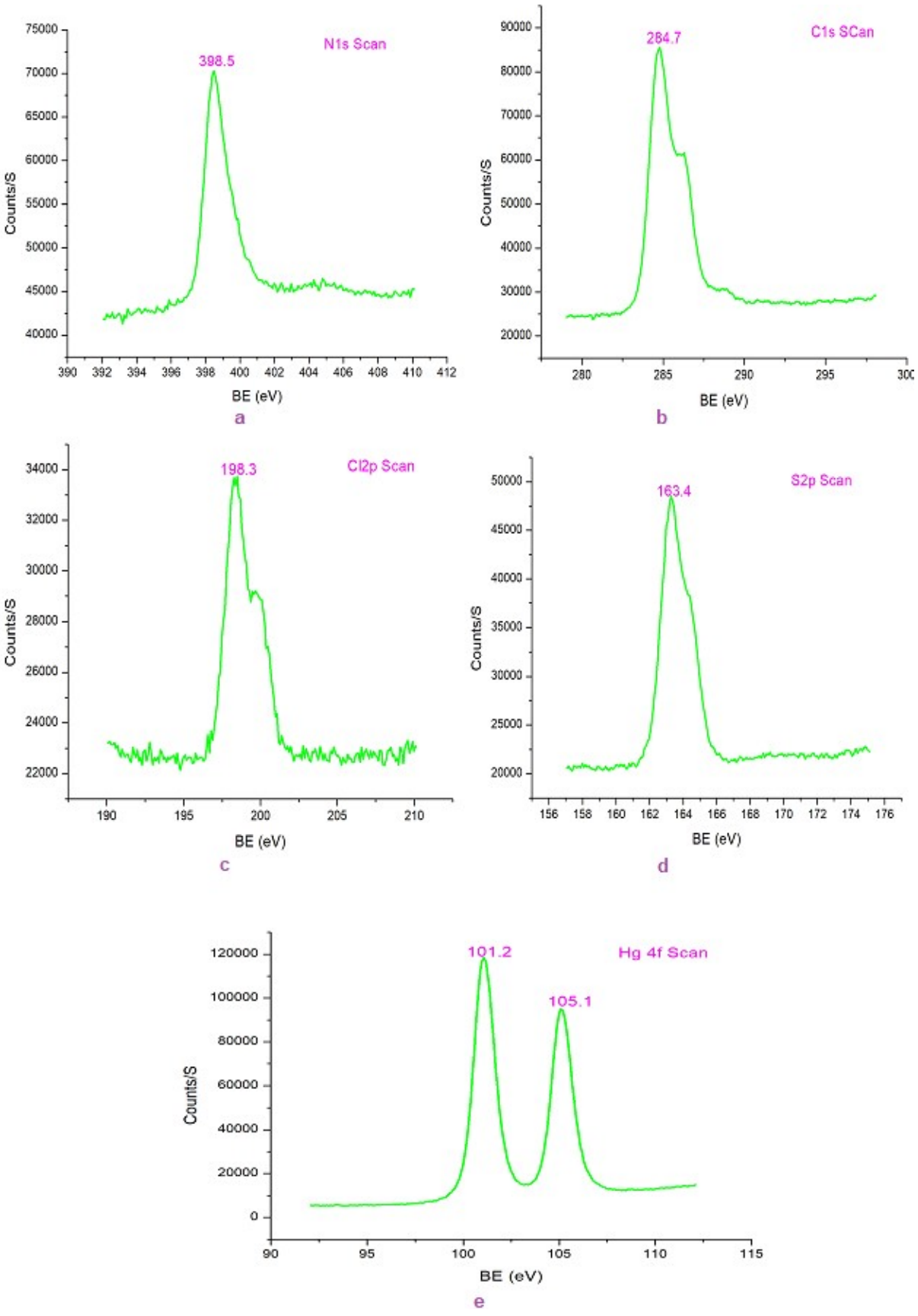

Fig.S12a-e XPS graphical representation for complex **1.**

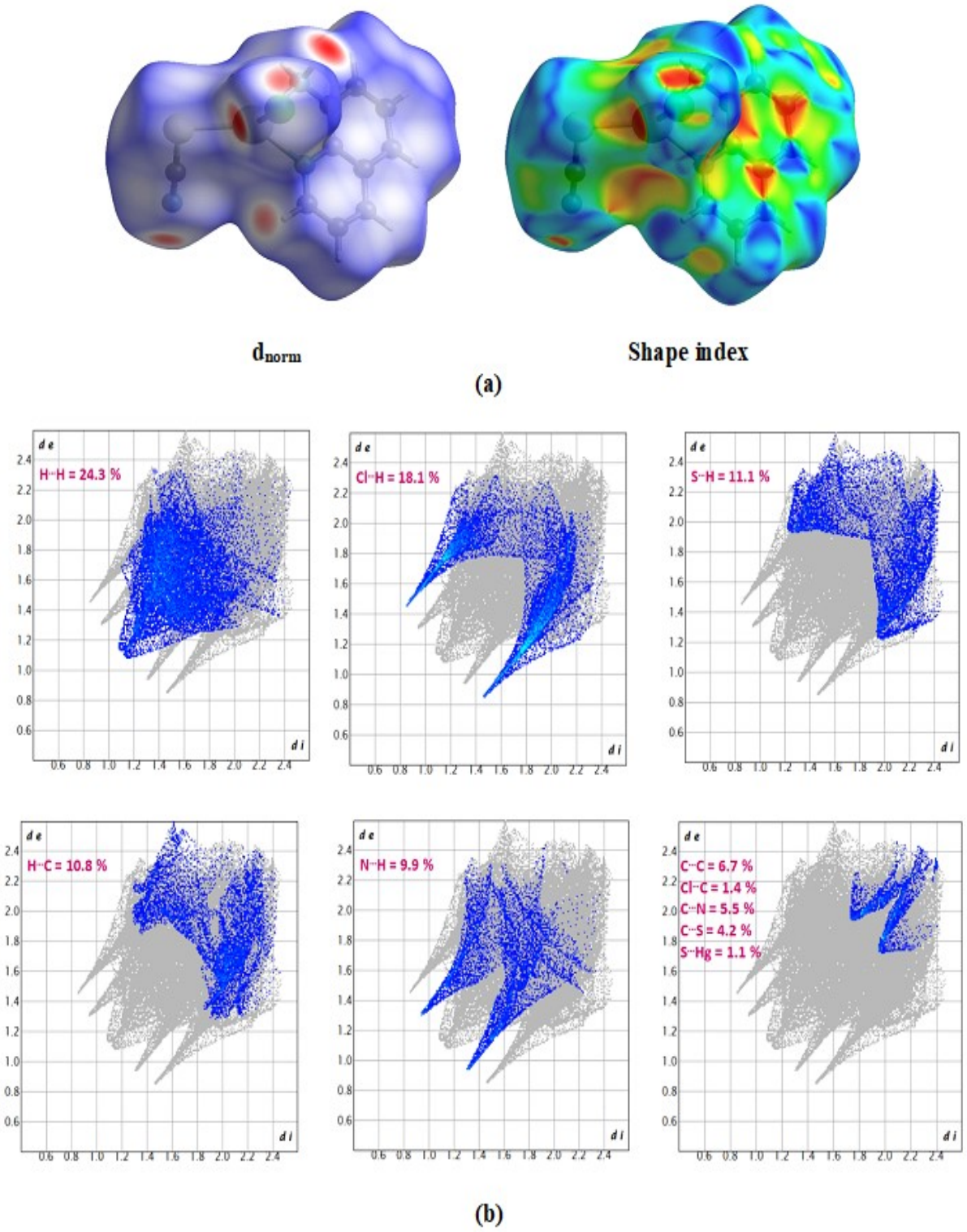

Fig.S13 Hirshfeld surface and 2D Fingerprints for complex **1 (**a, b).

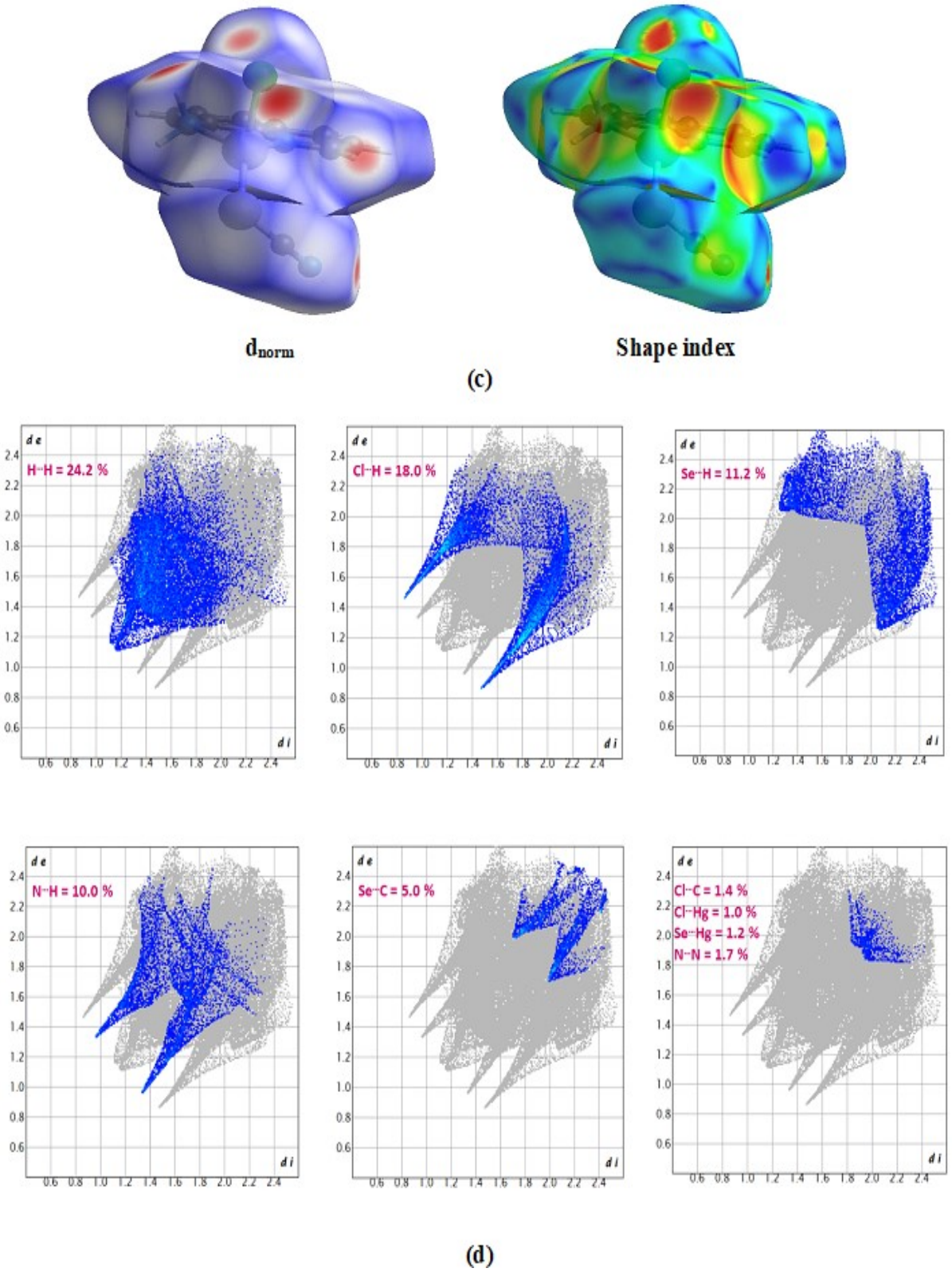

Fig. S14 Hirshfeld surface and 2D Fingerprints for complex **2 (**c, d).

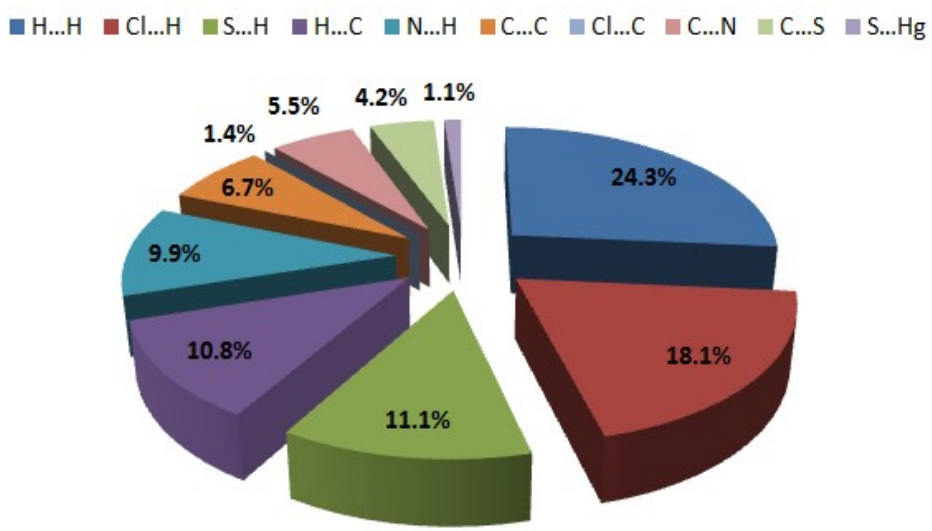

Fig.S14a Histogram showing the different percentage of HS contacts.

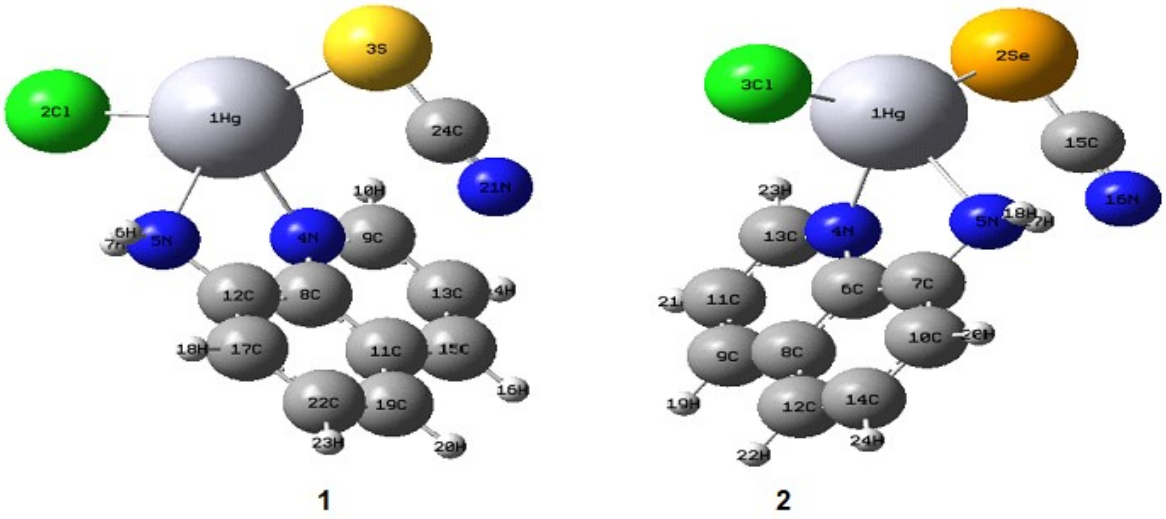

Fig.S15 DFT optimized the structure of the Hg(II) complexes.

References

S1 S. Hazra, D. J. Majumdar, A. Frontera, S. Roy, B. Gassoumi, H. Ghalla, and S. Dalai, *Crystal Growth & Des.,* 2024, **24**, 7246–7261.

S2 S. Hazra, D. J. Majumdar, J. E. Philip, B. Gassoumi, H. Ghalla, S. Roy, and S. Dalai, *J. Inorg. Organomet. Polym.,* (2024). https://doi.org/10.1007/s10904-024-03251-9.

S3 L. M. Yang, Y. Liu, L. M. Man, M J. R. Zhou, X. P. Liu, and C. L. Ni, *Vib. Spectrosc.,* 2017, **93,** 23-28.

S4 B. Abdelaziz, Z. Mazouz, B. Gassoumi, N. E1 Islam Boukortt, S. Patanè, and S. Ayachi, *J. Mol. Liq.,* 2024, **395 (1),** 123934.

S5 R. Kumar, A. Thakur, D. S. Chandra, A. K. Dhiman, P. K. Verma, and U. Sharma, *Coord. Chem. Rev.,* 2024, **499,** 215453.